Biochemical and Biophysical Research Communications 427 (2012) 677–681

Contents lists available at SciVerse ScienceDirect

Biochemical and Biophysical Research Communications

journal homepage: www.elsevier.com/locate/ybbrc

Recombinant proteins incorporating short non-native extensions may display increased aggregation propensity as detected by high resolution NMR spectroscopy

Serena Zanzoni, Mariapina D'Onofrio, Henriette Molinari, Michael Assfalg *

Department of Biotechnology, University of Verona, 37134 Verona, Italy

ARTICLE INFO

Article history:
Received 16 September 2012
Available online 1 October 2012

Keywords:
Recombinant protein
Aggregation
NMR spectroscopy
Bile acid binding protein
Protein sequence
Diffusion

ABSTRACT

The use of a recombinant protein to investigate the function of the native molecule requires that the former be obtained with the same amino acid sequence as the template. However, in many cases few additional residues are artificially introduced for cloning or purification purposes, possibly resulting in altered physico-chemical properties that may escape routine characterization. For example, increased aggregation propensity without visible protein precipitation is hardly detected by most analytical techniques but its investigation may be of great importance for optimizing the yield of recombinant protein production in biotechnological and structural biology applications.

In this work we show that bile acid binding proteins incorporating the common C-terminal LeuValProArg extension display different hydrodynamic properties from those of the corresponding molecules without such additional amino acids. The proteins were produced enriched in nitrogen-15 for analysis *via* heteronuclear NMR spectroscopy. Residue-specific spin relaxation rates were measured and related to rotational tumbling time and molecular size. While the native-like recombinant proteins show spin-relaxation rates in agreement with those expected for monomeric globular proteins of their mass, our data indicate the presence of larger adducts for samples of proteins with very short amino acid extensions. The used approach is proposed as a further screening method for the quality assessment of biotechnological protein products.

1. Introduction

The use of recombinant DNA technology for the expression of proteins in both prokaryotic and eukaryotic cells is a well-accepted technology [1]. The optimal design of an expression vector requires consideration of several practical needs, including the introduction of recognition sites for restriction enzymes or the incorporation of fusion partners [2]. Although it is recommended that the recombinantly expressed proteins lack any unnecessary flexible, non-structured tails, few non-native amino acid residues may unavoidably be present. Short amino acid extensions are often biologically inert, however retention of native activity may not necessarily imply that all native properties of the macromolecule are preserved.

As an example, a frequent application of the use of fusion partners is to provide an affinity tag that facilitates purification. The removal of tags is then performed with proteases, such as factor Xa or thrombin, able to recognize specific amino acid sequences that need to be purposely engineered [3]. A commonly used thrombin cleavage site is constituted by the LeuValProArg↓GlySer sequence, resulting in a LeuValProArg extension being left after proteolysis if introduced at the carboxy-terminus. A differential behavior between a recombinant protein incorporating a LeuValProArg tail and the corresponding native macromolecule has already been reported [4]. Recombinant human haptocorrin behaved as the native protein concerning its spectral properties and ability to recognize both cobalamin and its baseless analog cobinamide. Interestingly, however, the recombinant protein showed subtle changes in the binding kinetics that were attributed to a direct perturbation of the binding site produced by the presence of four excessive amino acids.

Particularly deceitful is the situation where the bulk protein molecules are folded and active, but they have altered hydrodynamic properties. Protein–protein aggregation resulting in stable adducts can be detected by routine analysis such as size-exclusion chromatography. However, reversible formation of supramolecular species may be difficult to capture but detrimental for the obtainment of pure monomeric protein samples. In addition, since dismal consequences of specific protein aggregates have been recognized as a major cause of a number of pathologies, including Alzheimer's

Abbreviations: BABP, bile acid binding protein; HSQC, heteronuclear single quantum coherence.

* Corresponding author. Address: Department of Biotechnology, University of Verona, Strada Le Grazie 15, 37134 Verona, Italy. Fax: +39 045 8027949.
E-mail address: michael.assfalg@univr.it (M. Assfalg).

0006-291X/$ - see front matter © 2012 Elsevier Inc. All rights reserved.
http://dx.doi.org/10.1016/j.bbrc.2012.09.121

and Parkinson's diseases [5,6], detailed characterization of this aspect should become mandatory for protein biopharmaceuticals [7].

The use of NMR spectroscopy to screen the quality of protein samples is already state-of-the-art in many research laboratories and has become an invaluable tool in large-scale structural genomics programs [8]. Indeed, heteronuclear 2D NMR experiments such as the ^{1}H, ^{15}N-HSQC provide, with a single experiment, a significant amount of information about protein foldedness, sample purity, conformational heterogeneity, and stability [9]. The huge versatility of the technique allows an ample variety of molecular characterizations to be performed. Several NMR parameters, such as the diffusion coefficient, nuclear Overhauser effect, transverse and longitudinal relaxation rates can detect perturbations in either translational or rotational diffusion with high sensitivity [10–13]. We show here, by measuring simple ^{15}N longitudinal relaxation time constants, that protein constructs differing for the introduction of one or few amino-acids at the N- or C-terminal ends display different aggregation propensities, thereby affecting the quality of the biotechnological product.

Bile acid binding proteins (BABPs) were chosen here to investigate hydrodynamic properties of recombinant products obtained from different expression constructs. These small globular cytosolic molecules are quite soluble, they can be produced in high yield *via* heterologous expression in *Escherichia coli* and have been well characterized in terms of structure, dynamics, and binding properties [14–20]. Protein aggregation phenomena have been reported to occur under partial denaturing conditions [21]. A convenient feature for the purpose of this study is that while displaying a variety of primary sequences, members of the BABP family show practically superimposable tertiary folds [18,22–25]. This notion allows to exclude that differences in molecular interactions are consequent of alternative conformations. In this work we have characterized the human ileal (hI-BABP), chicken ileal (cI-BABP), and chicken liver (cL-BABP) proteins.

2. Materials and methods

2.1. Cloning of BABP proteins

The DNA coding for cI-BABP, provided by P. Pesente (Tre Valli Laboratory, Verona, Italy) was obtained by reverse transcription from total RNA extracted from chicken ileum [19], PCR amplified using BamHI and SacI restriction enzymes and cloned into the expression vector pQE50 (Qiagen), which encodes a C-terminal His_6-tag (construct *1*, Fig. 1). To increase the yield of this soluble protein, the plasmid carrying the cI-BABP was mutated using the QuickChange® site-directed mutagenesis kit (Stratagene) inserting a stop codon after the sequence coding for the first four residues of the thrombin cleavage site in order to obtain the same tag that would have been found after proteolytic cut (construct *2*, Fig. 1). Due to the presence of an arginine in both the C-terminal tag and the four-residue N-terminal fragment, the predicted isoelectric point of cI-BABP was increased from the original value of 6.8–8.6. This feature allowed purifying the protein with ionic exchange chromatography, thus eliminating the thrombin cleavage step, which may cause protein precipitation [26]. A BamHI-SacI fragment containing the DNA sequence coding for cI-BABP was also cloned into a pET28 (Novagen) modified plasmid (without N-terminal His_6-tag). In the latter construct, a stop codon is inserted at the C-terminal end of the cI-BABP coding sequence (construct *3*, Fig. 1).

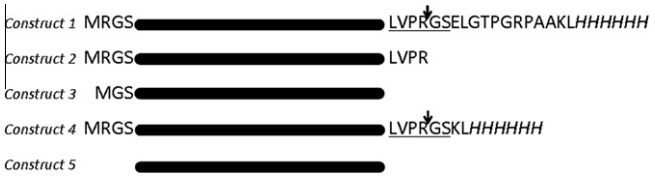

Fig. 1. Scheme of expression constructs used in this work. Construct *1*: the original sequence of cI-BABP in pQE50 plasmid with a short N-terminal sequence and a long C-terminal sequence containing the thrombin cleavage site and a His_6-tag. Construct *2*: sequence of cI-BABP in the same plasmid as construct *1*, with the short N-terminal tag and the C-terminal tag cut after the first four residues. Construct *3*: the sequence of cI-BABP in pET28 expressed without C-terminal tag. Construct *4*: sequence of hI-BABP cloned in pQE50 with N-terminal tag and His_6-tag at the C-terminus. Construct *5*: sequence of cL-BABP cloned in pET24 (from Ala1 to Val125) expressed without additional amino acids.

The plasmid with the gene coding for hI-BABP was purchased from Deutsches Ressourcenzentrum für Genomforschung GmbH (RZPD). The hI-BABP coding sequence used in this study differs from the one reported in the literature [14,27] for two polymorphisms corresponding to residues 32 (Arg/His) and 54 (Ser/Tyr). The DNA sequence encoding hI-BABP was PCR amplified generating a BamHI and HindIII restriction sites and cloned into pQE50 with a thrombin cleavage site before the C-terminal His_6-tag (construct *4*, Fig. 1), thus with the same extension tags as constructs *1* and *2*.

cL-BABP was expressed from the mutated pET24-cL-BABP H98Q construct (construct *5*, Fig. 1) not including any additional tag [28].

2.2. Protein expression and purification

Recombinant cI-BABP was expressed as soluble protein in *E. coli* SG cells (Qiagen) harboring the pQE50 plasmid (constructs *1* and *2*), or BL21 (DE3) cells (Stratagene) including the pET28 plasmid (construct *3*). For each strain, 1 L of M9 minimal medium was inoculated with 5 mL of a starter culture and incubated at 37 °C until cells reached an OD_{600} of 0.6. Protein expression was induced by addition of isopropylthiogalactopyranoside (IPTG) 0.5 mM and incubated overnight at 28 °C. The cells were harvested by centrifugation and resuspended in lysis buffer containing phenylmethanesulfonylfluoride (PMSF) as protease inhibitor. After sonication and centrifugation, the supernatant, containing the protein in soluble form, was loaded on a DEAE-cellulose (Whatman) anion exchange column equilibrated with 50 mM Tris acetate, pH 7.8. The same buffer was used for protein elution. Fractions containing cI-BABP were collected, concentrated and resolved on a Sephacryl S-100 HR (GE Healtcare). The protein was delipidated as described [18], the protein purity was verified by the presence of a single band on SDS–PAGE (Supplementary data Fig. S1) and by ^{1}H NMR.

The human protein was expressed inoculating an *E. coli* SG starter culture in M9 minimal medium, supplemented with ^{15}N ammonium chloride and ^{12}C- or ^{13}C-glucose for single or double-labeled protein. Due to the low level of solubility, we used a protocol of expression and purification from inclusion bodies. After overnight induction a 37 °C, the protein was refolded as described previously for some hI-BABP mutants [29]. After refolding, hI-BABP was purified *via* nickel-affinity chromatography with an imidazole gradient, followed by thrombin cleavage. The cleaved protein was resolved on a Superdex G75 column (GE Healtcare) and delipidated. Purification from inclusion bodies yielded >95% pure protein by SDS–PAGE analysis. The fold and stability were monitored by ^{1}H NMR.

Recombinant cL-BABP was expressed and purified as previously reported [28].

2.3. NMR experiments

NMR samples of chicken and human I-BABP were prepared by resuspending 0.4 mM protein in a buffer solution containing

20 mM sodium phosphate, 1 mM DTT, and 0.05% NaN_3, pH 6.5, in 90% H_2O/10% D_2O. A protein sample in phosphate buffer at pH 7.0 was employed for relaxation measurement of cL-BABP, while ^{15}N-ubiquitin was 1 mM in phosphate buffer, pH 5.8.

NMR spectra were recorded on a 600 MHz Bruker Avance III spectrometer equipped with cryogenic probe. The measurement temperature was 25 °C for all BABPs and 27 °C for ubiquitin.

Typical ^{1}H, ^{15}N-HSQC experiments were recorded with a data matrix consisting of 2048 (F2, ^{1}H) × 128 (F1, ^{15}N) complex points. The number of scans was 16 and the relaxation delay 1.5 s. Spectral windows of 9615 (F2) and 2189 (F1) Hz were used.

The backbone resonance assignment of uniformly ^{13}C- and ^{15}N-enriched hI-BABP was based on the analysis of HNCACB, CBCA(CO)NH, and ^{15}N-HSQC-NOESY heteronuclear NMR experiments, as well as on available data reported in [27].

Protein backbone ^{15}N-T_1 experiments were recorded on ^{15}N-labeled proteins. Experiments were performed in gradient-selected sensitivity-enhanced mode and in interleaved fashion, using a matrix of 2048 (^{1}H) × 128 (^{15}N) complex data-points for each relaxation delay and spectral widths of 13 and 33 ppm in the ^{1}H and ^{15}N dimensions, respectively. Optimal water signal suppression was obtained with a flip-back pulse. The recycle delay was 38 s. T_1 relaxation delays were 0.01, 0.18 (duplicate), 0.36, 0.54, 0.72, 0.90, 1.08, 1.26 (duplicate), 1.44 s.

Data were processed using TOPSPIN 2.1 (Bruker, Karlsruhe, Germany) and analyzed with the same software or with CARA [30]. Relaxation times T_1 were determined by fitting peak heights of respective experimental data sets to a single exponential decay using the computer program RELAXFIT [31]. Matlab 7.0 (Mathworks Inc.) and Origin 7.5 (Originlab) were used for graphing.

3. Results

3.1. Protein production

In this work we investigated the properties of BABPs produced as recombinant molecules expressed in *E. coli* using different constructs. cI-BABP was obtained from expression of either construct *2* or construct *3* (Fig. 1). The former construct encodes for a protein incorporating an N-terminal MRGS fragment and a C-terminal LVPR tail in addition to the native protein sequence. The corresponding protein, hereafter indicated cI-BABP^{LVPR}, has a predicted isoelectric point of 8.63 and nominal mass of 15152 Da (15335 Da if enriched in nitrogen-15). cI-BABP was also expressed from construct *3*, which encodes for a protein with an N-terminal MGS fragment and no C-terminal tail, simply referred to as cI-BABP.

hI-BABP was expressed from construct *4*, encoding for a C-terminal hexahistidine tag and a thrombin recognition site. The purified hI-BABP incorporates an N-terminal MRGS and a C-terminal LVPR chain and will be indicated as hI-BABP^{LVPR} as opposed to hI-BABP described in Refs. [14,27], produced without the LVPR tail. hI-BABP^{LVPR} has an isoelectric point of 6.91 and a molecular mass of 15194.

cL-BABP was produced with no additional tags compared to the native protein, its isoelectric point and molecular mass are 8.69 and 14079 Da.

Human ubiquitin (Ub) was also included in the study as it constitutes a common NMR standard with well-characterized properties. The protein, had no artificial terminal fragments, pI = 6.56, Mw = 8564.

Proteins for NMR analysis were all prepared as nitrogen-15-labeled molecules. For all protein samples ^{1}H-1D and ^{1}H, ^{15}N-HSQC 2D spectra were acquired to confirm sample purity and structural integrity. Well-dispersed cross-peaks were observed in all 2D spectra (Supplementary data Fig. S2).

3.2. Residue-specific NMR signal assignment

The sequence-specific backbone resonance assignment for hI-BABP^{LVPR} was established, using 3D triple-resonance experiments, for 125 of the 126 non-proline residues of the native protein sequence. Only minor differences were found in peak positions compared to those reported by Horváth et al. [27], confirming that the proteins used in the two studies have the same structure.

The residue-specific assignment for cI-BABP^{LVPR} has been previously established. Starting from this data the amide H and N resonances of cI-BABP were assigned by visual comparison of the corresponding ^{1}H, ^{15}N-HSQC spectra (Supplementary data Fig. S2). The major differences correspond to signals from residues positioned near the N- or C-termini and reflect local changes in their chemical environment. The assignment of HN resonances of cL-BABP was previously reported [28].

The assignment of Ub was made by reference to entry 17769 in the Biological Magnetic Resonance Data Bank without further confirmation.

3.3. Nitrogen-15 relaxation analysis

Longitudinal ^{15}N spin relaxation times, ^{15}N-T_1, were measured for proteins Ub, hI-BABP^{LVPR}, cI-BABP, cI-BABP^{LVPR}, and cL-BABP. The values obtained for all identified N_H atoms of Ub are plotted as a function of primary sequence in Fig. 2. The values taken from Tjandra et al. [32] are reported for comparison and indicate perfect agreement between the two studies. Fluctuations along the protein sequence reflect contributions of local internal motions of the N-H vectors that are faster than the overall rotational tumbling. Lower values correspond to rigid protein regions and are determined from overall rotational motion. The correlation time for the global rotation, T_R, is in turn related to molecular mass, such that ^{15}N-$T_1 \propto \tau_R \propto$ Mw. The theoretical dependence is plottedin Fig. 3 for molecular masses up to 20 kDa, considering that $\tau_R \sim 0.5 \times$ Mw at ambient temperature. This curve was earlier introduced as a molecular weight calibration 'ruler' for polyubiquitin chains [33]. Experimental data may be displayed on the diagram to evaluate the apparent mass of a protein sample for which relaxation data have been measured. The experimental data for the standard NMR sample Ub allows predicting a molecular mass that is in good agreement with the actual value, confirming that the protein is monomeric and freely rotating in solution.

NMR relaxation data for hI-BABP have been reported earlier and a ^{15}N-T_1 average value of 0.605 ± 0.038 s was found [27]. These data, together with transverse relaxation and heteronuclear NOE data, were analyzed in detail allowing to determine a motional correlation time T_R of 6.8 ns, a reasonable value based on molecular size. We have repeated the ^{15}N-T_1 measurements on hI-BABP^{LVPR} and they appeared quite different from those reported in [27], resulting in an average value of 0.745 ± 0.037 s (Fig. 4A). The

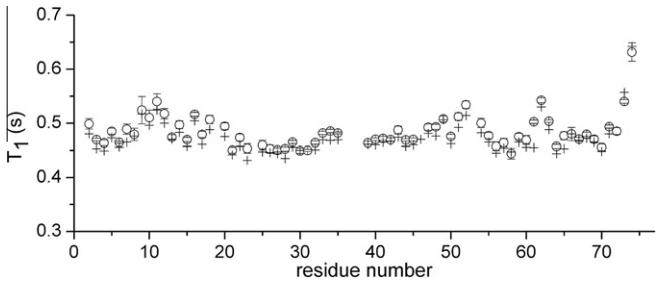

Fig. 2. Residue-specific ^{15}N-T_1 values of Ub. ○, values measured in this work, error bars refer to fitting errors; +, values obtained from [32]. Data were collected at 600.13 MHz proton Larmor frequency and 27 °C.

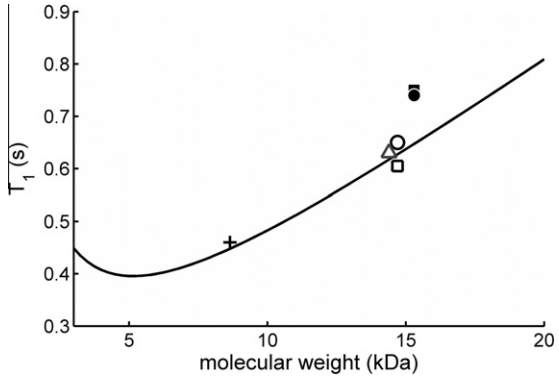

Fig. 3. Molecular weight dependence of ^{15}N-T_1. The line represents the predicted curve, assuming isotropic rigid rotational tumbling, linear dependence of the rotational correlation time from the molecular weight, and considering a proton Larmor frequency of 600.13 MHz and 25 °C. Symbols correspond to experimental data, determined as the average of T_1 values for all residues in secondary structure elements. +, Ubiquitin; ●, cI-BABP^{LVPR}; ○, cI-BABP; ■, hI-BABP^{LVPR}; □, hI-BABP; Δ, cL-BABP.

observed increase in relaxation time cannot be ascribed to a difference in mass determined by few additional amino acids and it can be concluded that protein–protein interactions restrict rotational motion.

In order to verify this hypothesis with a different protein, relaxation measurements were performed on cI-BABP and cI-BABP^{LVPR}, displaying a sequence identity of 62% with hI-BABP. ^{15}N-T_1 values are plotted as a function of protein sequence in Fig. 4B. Again it can be easily observed that the experimental data are quite different between the two protein samples, with average ^{15}N-T1 values of 0.651 and 0.740 s found for cI-BABP and cI-BABP^{LVPR}, respectively. These numbers, reported in Fig. 3, indicate a correct predicted molecular mass for cI-BABP, while the predicted mass of cI-BABP^{LVPR} appears ~2 kDa larger than expected.

We finally analyzed a third member of the BABP family, cL-BABP, displaying a sequence identity of 42% to cI-BABP and a very similar tertiary fold. The protein was produced with no artificial terminal residues and the corresponding ^{15}N-T_1 values are plotted in Fig. 4C. The striking analogy between the relaxation data of cI-BABP and cL-BABP, despite the significantly different amino acid composition, supports the conclusion that the different hydrodynamic behavior of hI-BABP^{LVPR} and cI-BABP^{LVPR} must arise from the N- or C-termini.

It appears that either the N-terminal additional Arg residue or the C-terminal LeuValProArg tail promote formation of high molecular weight aggregates. The latter species are probably transient in nature, as no further indication of aggregation is found from chromatograms acquired during purification. A positively charged Arg side chain at both termini discriminates cI-BABP^{LVPR} from cI-BABP, possibly resulting in intermolecular electrostatic interactions. Alternatively, the apolar LeuValPro amino acid triplet may establish hydrophobic interactions.

4. Discussion

In this work the longitudinal ^{15}N-spin relaxation time constants for BABP proteins produced from different recombinant expression constructs were measured and compared. Proteins incorporating few additional artificial residues at the N-terminus and C-terminus display relaxation properties that correspond to molecules of significantly larger size, suggestive of increased aggregation propensity. The observed differential behavior could be detected thanks to the sensitivity of the NMR method to the occurrence of transient interactions that may escape other common routine biochemical analyses.

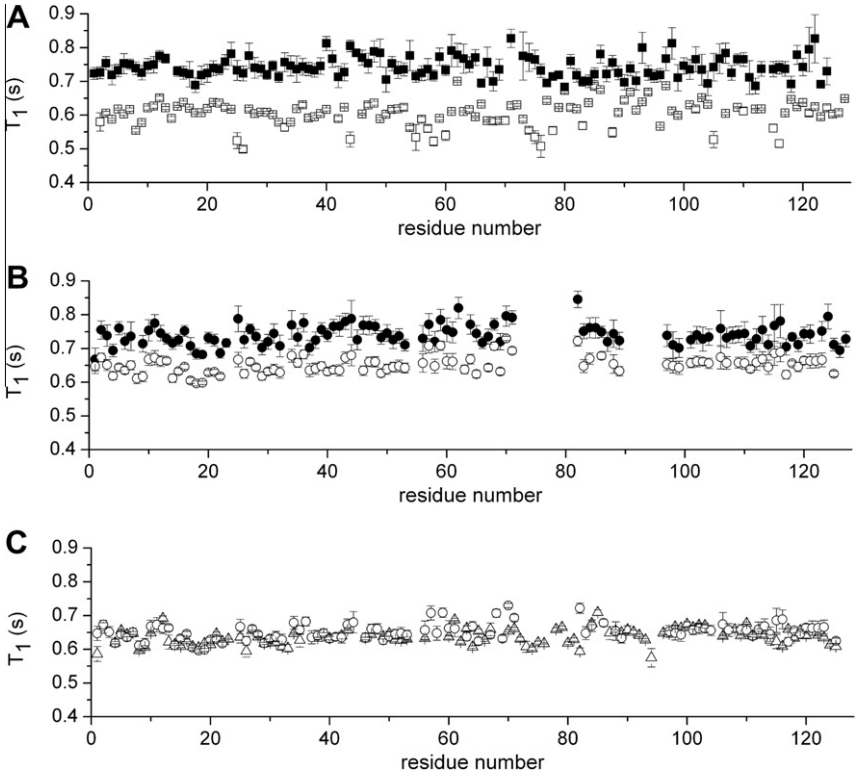

Fig. 4. Residue-specific ^{15}N-T_1 values of BABPs. (A) ■, hI-BABP^{LVPR}; □, hI-BABP: values obtained from Horváth et al. [27]. (B) ●, cI-BABP^{LVPR}; ○, cI-BABP. (C) Δ, cL-BABP; ○, cI-BABP. Error bars refer to fitting errors. Data were collected at 600.13 MHz proton Larmor frequency and 25 °C.

It should be noted that in alternative to the measurement of residue-specific relaxation times, ^{15}N-T_1 values can also be derived from the ratios between the total integrals of the overall envelopes of 1D spectra recorded with different delays. However, the analysis of relaxation data for all amino acids has the advantage that local differences in mobility can be detected, for example highlighting increased dynamics in specific protein regions or the partial loss of secondary structure. The method can also be made more accurate by including a more detailed description of the predicted hydrodynamic behavior of the investigated protein, taking into consideration motional anisotropy and deconvoluting local dynamics as determined from additional NMR relaxation experiments. The transverse spin relaxation rate can also be used as an indicator of rotational tumbling and molecular size, however with the disadvantage that it may be affected by chemical exchange [34]. Finally, translational diffusion can also be monitored by NMR and has often been used to evaluate molecular sizes [35]. The drawbacks of the latter method reside in more demanding requirements in terms of accurate instrumental set-up and temperature stabilization, the possibility of artifacts originating from non-exponential decays, and the loss of sequence-specific information.

The relevance of performing an experimental evaluation of molecular hydrodynamic properties also resides in the fact that structural data about terminal chains are often incomplete or unreliable, preventing an accurate computational prediction of the aggregation propensity promoted by these elements [36].

The detection of self-aggregation by recombinant proteins bearing even small artificial amino acid extensions is of great value in many biotechnological/industrial applications and may lead to optimized construct design.

Acknowledgment

This work was supported by the Ministero dell'Istruzione, dell'Università e della Ricerca (FIRB, Futuro in Ricerca, grant no. RBFR08R7OU).

Appendix A. Supplementary data

Supplementary data associated with this article can be found, in the online version, at http://dx.doi.org/10.1016/j.bbrc.2012.09.121.

References

[1] F. Baneyx, Recombinant protein expression in *Escherichia Coli*, Curr. Opin. Biotechnol. 10 (1999) 411–421.
[2] S. Zerbs, A.M. Frank, F.R. Collart, Bacterial systems for production of heterologous proteins, Meth. Enzymol. 463 (2009) 149–168.
[3] D.S. Waugh, An overview of enzymatic reagents for the removal of affinity tags, Protein Expr. Purif. 80 (2011) 283–293.
[4] E. Furger, S.N. Fedosov, D. Launholt Lildballe, R. Waibel, R. Schibli, E. Nexo, et al., Comparison of recombinant human haptocorrin expressed in human embryonic kidney cells and native haptocorrin, PLoS ONE 7 (2012) e37421.
[5] H.-J. Lee, Membrane-bound alpha -synuclein has a high aggregation propensity and the ability to seed the aggregation of the cytosolic form, J. Biol. Chem. 277 (2001) 671–678.
[6] C.L. Masters, G. Simms, N.A. Weinman, G. Multhaup, B.L. McDonald, K. Beyreuther, Amyloid plaque core protein in Alzheimer disease and Down syndrome, Proc. Natl. Acad. Sci. USA 82 (1985) 4245–4249.
[7] E. García-Fruitós, E. Vazquez, N. Gonzalez-Montalbán, N. Ferrer-Miralles, A. Villaverde, Analytical approaches for assessing aggregation of protein biopharmaceuticals, Curr. Pharm. Biotechnol. 12 (2011) 1530–1536.
[8] G.T. Montelione, D. Zheng, Y.J. Huang, K.C. Gunsalus, T. Szyperski, Protein NMR spectroscopy in structural genomics, Nat. Struct. Biol. 7 (Suppl.) (2000) 982–985.
[9] M. Bieri, A.H. Kwan, M. Mobli, G.F. King, J.P. Mackay, P.R. Gooley, Macromolecular NMR spectroscopy for the non-spectroscopist: beyond macromolecular solution structure determination, FEBS J. 278 (2011) 704–715.
[10] J. Cavanagh, Protein NMR Spectroscopy Principles and Practice, Academic Press, Amsterdam, Boston, 2007.
[11] R. Ishima, D.A. Torchia, Protein dynamics from NMR, Nat. Struct. Biol. 7 (2000) 740–743.
[12] B. Zambelli, N. Cremades, P. Neyroz, P. Turano, V.N. Uversky, S. Ciurli, Insights in the (un)structural organization of Bacillus pasteurii UreG, an intrinsically disordered GTPase enzyme, Mol Biosyst. 8 (2012) 220–228.
[13] P. Bernadó, J. García de la Torre, M. Pons, Macromolecular crowding in biological systems: hydrodynamics and NMR methods, J. Mol. Recognit. 17 (2004) 397–407.
[14] G.P. Tochtrop, K. Richter, C. Tang, J.J. Toner, D.F. Covey, D.P. Cistola, Energetics by NMR: site-specific binding in a positively cooperative system, Proc. Natl. Acad. Sci. USA 99 (2002) 1847–1852.
[15] H.L. Monaco, Review: the liver bile acid-binding proteins, Biopolymers 91 (2009) 1196–1202.
[16] M. Trauner, J.L. Boyer, Bile salt transporters: molecular characterization, function, and regulation, Physiol. Rev. 83 (2003) 633–671.
[17] T. Eliseo, L. Ragona, M. Catalano, M. Assfalg, M. Paci, L. Zetta, et al., Structural and dynamic determinants of ligand binding in the ternary complex of chicken liver bile acid binding protein with two bile salts revealed by NMR, Biochemistry 46 (2007) 12557–12567.
[18] S. Tomaselli, M. Assfalg, K. Pagano, C. Cogliati, S. Zanzoni, H. Molinari, et al., A disulfide bridge allows for site-selective binding in liver bile acid binding protein thereby stabilising the orientation of key amino acid side chains, Chem. Eur. J. 18 (2012) 2857–2866.
[19] M. Guariento, D. Raimondo, M. Assfalg, S. Zanzoni, P. Pesente, L. Ragona, et al., Identification and functional characterization of the bile acid transport proteins in non-mammalian ileum and mammalian liver, Proteins 70 (2008) 462–472.
[20] M. D'Onofrio, E. Gianolio, A. Ceccon, F. Arena, S. Zanzoni, D. Fushman, et al., High relaxivity supramolecular adducts between human-liver fatty-acid-binding protein and amphiphilic Gd(III) complexes: structural basis for the design of intracellular targeting MRI probes, Chem. Eur. J. 18 (2012) 9919–9928.
[21] M. D'Onofrio, L. Ragona, D. Fessas, M. Signorelli, R. Ugolini, M. Pedò, et al., NMR unfolding studies on a liver bile acid binding protein reveal a global two-state unfolding and localized singular behaviors, Arch. Biochem. Biophys. 481 (2009) 21–29.
[22] A.W. Zimmerman, J.H. Veerkamp, New insights into the structure and function of fatty acid-binding proteins, Cell. Mol. Life Sci. 59 (2002) 1096–1116.
[23] S. Capaldi, M. Guariento, M. Perduca, S.M. Di Pietro, J.A. Santomé, H.L. Monaco, Crystal structure of axolotl (*Ambystoma mexicanum*) liver bile acid-binding protein bound to cholic and oleic acid, Proteins 64 (2006) 79–88.
[24] S. Capaldi, G. Saccomani, D. Fessas, M. Signorelli, M. Perduca, H.L. Monaco, The X-ray structure of zebrafish (*Danio rerio*) ileal bile acid-binding protein reveals the presence of binding sites on the surface of the protein molecule, J. Mol. Biol. 385 (2009) 99–116.
[25] S. Zanzoni, M. Assfalg, A. Giorgetti, M. D'Onofrio, H. Molinari, Structural requirements for cooperativity in ileal bile acid-binding proteins, J. Biol. Chem. 286 (2011) 39307–39317.
[26] M. Guariento, M. Assfalg, S. Zanzoni, D. Fessas, R. Longhi, H. Molinari, Chicken ileal bile-acid-binding protein: a promising target of investigation to understand binding co-operativity across the protein family, Biochem. J. 425 (2010) 413–424.
[27] G. Horváth, P. Király, G. Tárkányi, O. Toke, Internal motions and exchange processes in human ileal bile acid binding protein as studied by backbone (15)N nuclear magnetic resonance spectroscopy, Biochemistry 51 (2012) 1848–1861.
[28] S. Tomaselli, L. Ragona, L. Zetta, M. Assfalg, P. Ferranti, R. Longhi, et al., NMR-based modeling and binding studies of a ternary complex between chicken liver bile acid binding protein and bile acids, Proteins 69 (2007) 177–191.
[29] O. Toke, J.D. Monsey, G.T. DeKoster, G.P. Tochtrop, C. Tang, D.P. Cistola, Determinants of cooperativity and site selectivity in human ileal bile acid binding protein, Biochemistry 45 (2006) 727–737.
[30] R.L.J. Keller, The Computer Aided Resonance Assignment Tutorial, CANTINA, Goldau, CH, 2004.
[31] D. Fushman, S. Cahill, D. Cowburn, The main-chain dynamics of the dynamin pleckstrin homology (PH) domain in solution: analysis of 15N relaxation with monomer/dimer equilibration, J. Mol. Biol. 266 (1997) 173–194.
[32] N. Tjandra, S.E. Feller, R.W. Pastor, A. Bax, Rotational diffusion anisotropy of human ubiquitin from 15N NMR relaxation, J. Am. Chem. Soc. 117 (1995) 12562–12566.
[33] R. Varadan, M. Assfalg, D. Fushman, Using NMR spectroscopy to monitor ubiquitin chain conformation and interactions with ubiquitin-binding domains, Meth. Enzymol. 399 (2005) 177–192.
[34] R. Ishima, D.A. Torchia, Estimating the time scale of chemical exchange of proteins from measurements of transverse relaxation rates in solution, J. Biomol. NMR 14 (1999) 369–372.
[35] A. Dehner, H. Kessler, Diffusion NMR spectroscopy: folding and aggregation of domains in p53, Chembiochem 6 (2005) 1550–1565.
[36] V. Castillo, R. Graña-Montes, R. Sabate, S. Ventura, Prediction of the aggregation propensity of proteins from the primary sequence: aggregation properties of proteomes, Biotechnol. J. 6 (2011) 674–685.